Article

Application of Inelastic Method and Its Comparison with Elastic Method for the Assessment of In-Box LOCA Event on EU DEMO HCPB Breeding Blanket Cap Region

Anoop Retheesh * , **Francisco A. Hernández and Guangming Zhou**

Karlsruhe Institute of Technology (KIT), Institute for Neutron Physics and Reactor Technology (INR), Hermann-von-Helmholtz-Platz 1, 76344 Eggenstein-Leopoldshafen, Germany; francisco.hernandez@kit.edu (F.A.H.); guangming.zhou@kit.edu (G.Z.)
* Correspondence: anoop.retheesh@kit.edu

Abstract: The Helium Cooled Pebble Bed (HCPB) breeding blanket, being developed by the Karlsruhe Institute of Technology (KIT) and its partners is one of the two driver blanket candidates to be selected for the European demonstration fusion power plant (EU DEMO). The in-box Loss of Coolant Accident (LOCA) is a postulated initiating event of the breeding blanket (BB) that must be accounted within the design basis. In this paper, the BB cap region is analyzed for its ability to withstand an in-box LOCA event. Initially, an assessment is performed using conventional elastic design codes for nuclear pressure vessels. However, it is thought that the elastic rules are not 'equipped' to assess the material damage modes which are essentially inelastic. Therefore, a non-linear inelastic analysis is further performed to better understand the damage in the material. Two predominant inelastic failure modes are thought to be relevant and addressed: *exhaustion of ductility* and *plastic flow localization.* While the design of HCPB BB has been predominantly based on the elastic design-by-analysis studies, results from the present study show that the elastic rules may be overly conservative for the given material and loading and could lead to inefficient designs. To our knowledge, this study is the first attempt to investigate the structural integrity of the European DEMO blankets under in-box LOCA conditions using the inelastic methods.

Keywords: EU DEMO; breeding blanket; LOCA; thermomechanical assessment; design-by-analysis; exhaustion of ductility; plastic flow localization; Eurofer97

1. Introduction

The EU DEMO denotes a crucial step between the International Thermonuclear Experimental Reactor (ITER) and the commercial generation of fusion power in Europe [1]. The HCPB breeding blanket is one of the two "driver" blanket concepts being considered for the EU DEMO [2]. The reference structural material for EU DEMO blankets is a Reduced Activation Ferritic-Martensitic (RAFM) steel: Eurofer97, which is capable of withstanding high neutron irradiation with low-activation. While for ITER, due to its experimental nature, an austenitic stainless steel type 316L(N)-IG is used as the structural material for the blankets is [3]. Figure 1 shows a brief overview of the present HCPB BB concept within the DEMO tokamak. Each BB segment consists of a breeder zone volume formed between a *first wall* and a *backplate,* which is supported by a *back supporting structure* (BSS). The breeder zone is filled with a hexagonal arrangement of *pressure tubes* connecting the *first wall* and the *backplate* and acting as radial stiffeners. The ceramic breeder material (Li_4SiO_4 + 35% mol Li_2TiO_3) in the form of a pebble bed is filled inside *breeder pins* and inserted into each of the *pressure tubes*. Further, the *pressure tubes* are surrounded by hexagonally shaped (prismatic) *neutron multiplier blocks* (NMB) made up of Beryllium alloy ($Be_{12}Ti$). More details of the present HCPB BB architecture can be found in [4].

Several HCPB BB concepts were extensively investigated using linear design-by-analysis methods with respect to codes and standards over the last decade [5–14]. Additionally, a few studies employed non-linear methods to conduct the failure analysis under normal operation (NO) conditions [15–17]. In-box LOCA is an identified design basis accident scenario [13,14,18] for the BB, in which the blanket box has to withstand the pressure exerted by the leakage of high-pressure coolant. The structural assessments of the HCPB breeding blanket under the in-box LOCA conditions are carried out in [5,9,14].
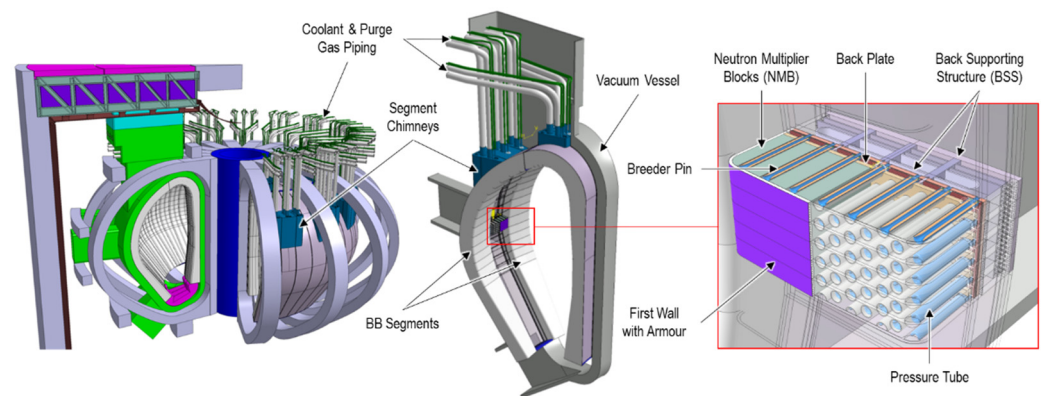
Figure 1. HCPB BB concept within the DEMO tokamak.

In contrast to the breeding zone at other regions, the cap region of the BB is considered predominantly a structural element, which does not contribute largely to tritium breeding. Therefore, the design of this region is oriented towards its structural strength and stiffness; while the breeding zone structural material has to be minimized to reduce the neutronic parasitic absorption. Consequently, the LOCA instead of the NO condition is considered as the design driver of the cap region. In this paper, the analysis is focused on the structural integrity of the BB cap region under the thermo-mechanical loading from an in-box LOCA event.

The elastic design-by-analysis codes and standards with the relatively large safety factors are thought of as a conservative criteria. However, it has been reported in [19] that the elastic rules failed to predict the failure due to non-standard loading on a pressure vessel, which could only be successfully predicted by the nonlinear elastoplastic analysis. The ductile material failure mechanism is essentially inelastic and nonlinear, while the elastic design codes are evolved from a linear, single-strength concept that does not account for the plastic deformation or its growth history [20]. It is reasoned in [21,22] that elastoplastic methods may be especially significant for the fusion community where non-standard components and construction are prevalent; in which the actual stresses may bear little resemblance to that predicted by the elastic rules. However, within the European fusion community, specific design criteria for the DEMO in-vessel components are under development and in early stages. For irradiated structures subjected to monotonic loading, the nuclear components design codes RCC-MRx [23] and SDC-IC [24] define two potential failure modes due to reduced ductility: Immediate plastic flow localization (IPFL) and Immediate local fracture due to exhaustion of ductility (ILFED). For DEMO divertor plasma-facing components, the IPFL is not considered as a potential failure mechanism for inelastic assessment because it is argued that the flow localization helps in strain redistribution and the ultimate failure will be captured by the ILFED criteria [21]. However, since the irradiated Eurofer retains considerable durability after necking, IPFL is considered the main concern for Eurofer instead of ILFED [23,25]. For BB's first wall, IPFL was the criteria used for the inelastic assessment in [17].

It is explained in [25] that the IPFL is related to the uniform elongation of the material and the ILFED to its total elongation. The uniform elongation indicates the limit of the force that the structure can handle, and the total elongation is the limit of the strain/displacement

that can be developed in a structure. Therefore, it can be realized that the IPFL is the relevant criteria for force-limited failures (due to primary loads) that can occur in the structure, whereas ILFED is the criteria for displacement-limited (due to secondary loads) failures. It is thought that the assessment with respect to any one of these criteria alone may not give a complete picture of the reliability of the design. For example, if the plastic instability is reached at any point in the structure, a slight further increase in primary loads can cause failure by rapidly consuming the ductility. Likewise, even if the primary loads are not causing the plastic instability, the secondary loading like thermal expansion can cause the structure to fail, by straining the structure beyond its total elongation point. Hence, in this paper, the inelastic assessment is carried out against both IPFL and ILFED criteria.

2. Materials and Methods

For the thermo-mechanical assessment of the BB cap region, LOCA pressure (primary) and thermal (secondary) loads were considered; inertial loads were assumed to be negligible and not considered. The procedure involved two analyses: at first, a steady-state thermal analysis is carried out corresponding to the normal operation (NO) to calculate the temperature distribution of the structure. Next, a linear-elastic static structural analysis is carried out with the temperature distribution of the structure obtained from the previous thermal analysis. The static-structural analysis is further repeated using the inelastic (incorporating material and geometric nonlinearities) method, and the results are then assessed and compared.

2.1. Thermal Analysis

By taking advantage of quasi-symmetry, only a half portion of the BB cap region is considered for the analysis. The analysis domain with major components is presented in Figure 2. For the sake of simplicity, convection due to the helium purge gas within the cap region and radiation from the NMB to their environment are assumed negligible. The following thermal loads and boundary conditions were applied.

- Plasma heat flux on the plasma-facing surface;
- Nuclear heating as spatially varying heat generation within each material;
- Helium coolant flow modelled as a 1-dimensional fluid flow with a constant, average heat transfer coefficient;
- Bulk helium coolant temperatures assumed as uniform ambient temperatures at the corresponding surfaces with conservative heat transfer coefficients;
- Bonded thermal contact defined between all surfaces that are in contact with each other;
- Constant gap thermal conductance value corresponding to the thermal conductivity of helium at relevant pressure is used to define thermal contact between closely spaced surfaces;
- Symmetry boundary conditions on the boundary section surfaces.

2.2. Linear-Elastic Structural Analysis

The structural analysis is carried out with primary and secondary loading, as required for the assessment under design codes. Only structural components of the cap region with Eurofer material are included in the analysis. As the primary load, a pressure of 9.2 MPa (design pressure of 8 MPa + 15% to account for uncertainties) is applied on all the surfaces in contact with the coolant and the purge gas after an in-box LOCA occurs. Thermal expansion due to the temperature distribution on the structural material obtained from the thermal analysis constituted the secondary load. Bonded contacts are defined between the components representing the welded regions. As boundary conditions, frictionless support is applied on the poloidal direction and the symmetry boundary condition is applied on the toroidal direction, on the corresponding section surfaces. Furthermore, an edge on the BSS is radially constrained, thus making the model fully constrained for the static structural analysis. The analysis domain with highlighted boundary conditions is shown in Figure 3.

(**a**)

(**b**)
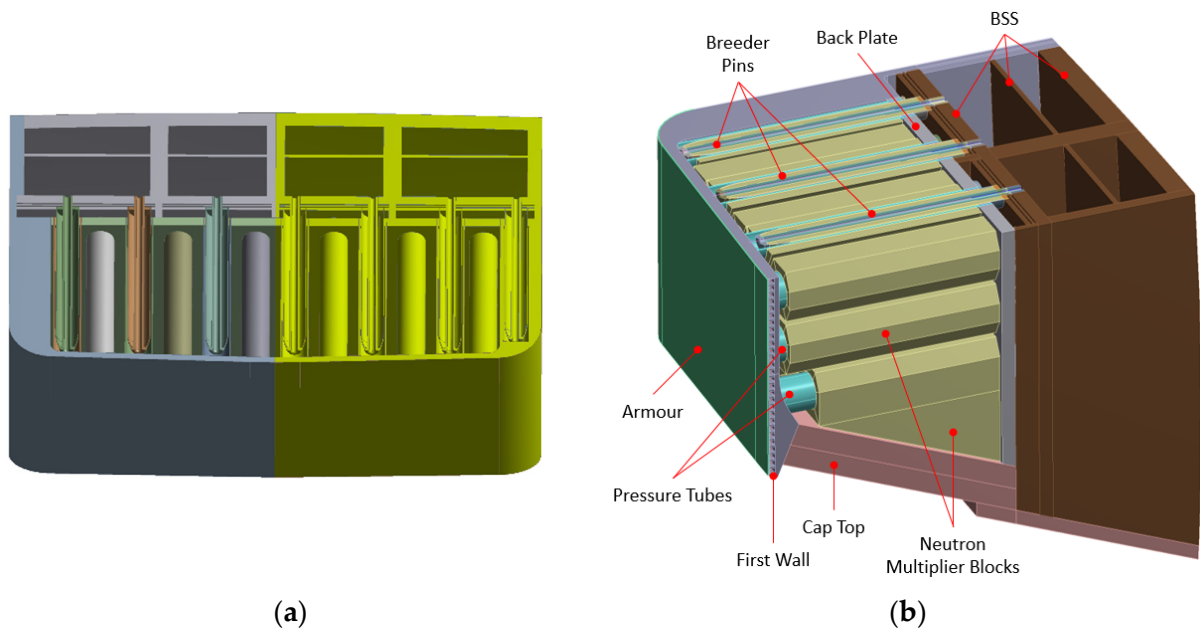
Figure 2. (**a**) HCPB BB cap region with highlighted symmetry section. (**b**) Symmetry section considered for simulation.
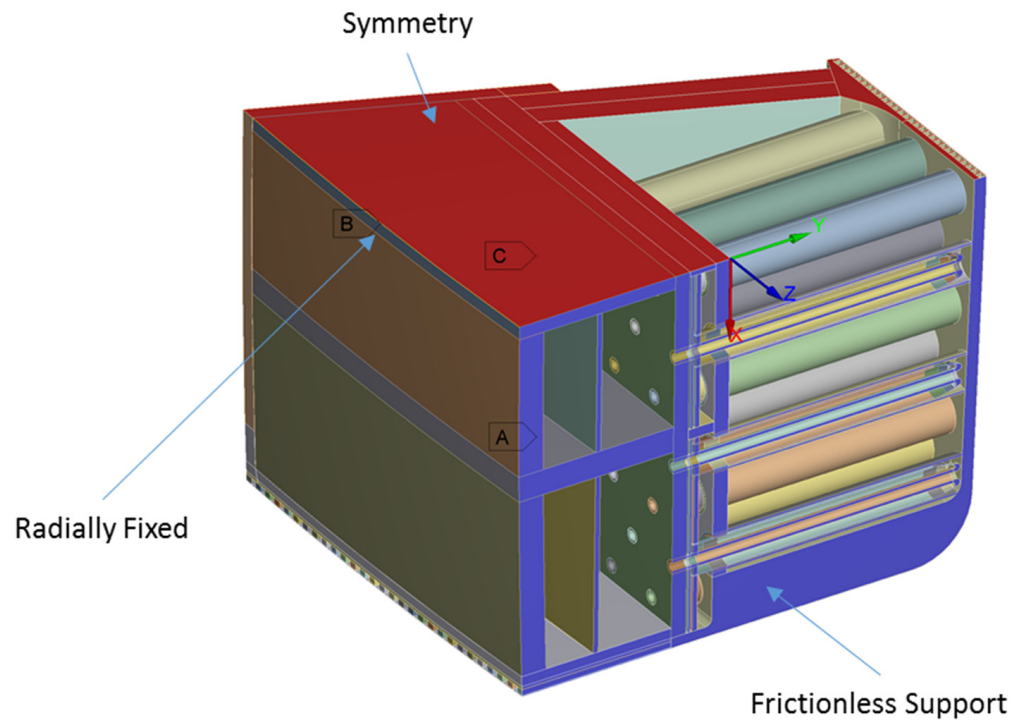
Figure 3. Static-structural analysis domain and boundary conditions.

2.3. Assessment according to Elastic Analysis Criteria

For the purpose of this work, the in-box LOCA is considered a design-basis accident, which should be assessed under Level-D criteria [14]. Hence, the failure is assessed with respect to two predominant modes that are thought to be relevant: the IPFL and the ILFED. The SDC-IC and RCC MRx recommend the following criteria to prevent IPFL failure mode [23–25].

$$\overline{P_L + Q_L} \ \leq \ S_{em} \ (RCC - MRx) \ or \ \overline{P_L + Q_L} \ \leq \ S_e \ (SDC - IC)$$

where P_L and Q_L are the primary and secondary local membrane stress, respectively, and S_{em} or S_e is the allowable elastic stress limit for the material dependent on the temperature and neutron fluence. This limit is defined in different ways as per both the codes, and the Level-D limit is further derived using a lower safety factor. From [25], it can be seen that the limit values estimated according to SDC-IC are conservative compared to those according to RCC-MRx at temperatures above 350 °C, the usual operating temperature range of HCPB BB. This is due to the difference in the way of accounting for the uniform elongation of the material within the definition of the stress limits. In order to be conservative, the stress limit values according to SDC-IC criteria are used for the assessment of IPFL failure mode in this work. The SDC-IC defines the stress limit S_e as a function of the tensile strength (S_u), which is dependent on irradiation and temperature; as well as the uniform strain for uniform strain values greater than 2%. Since irradiated Eurofer97 has uniform strain values less than 2% in the expected operating temperature range of HCPB BB (350 °C to 600 °C), it is decided to ignore the dependence on it. Furthermore, since the limit values apply throughout the lifetime with a range of irradiation, the minimum tensile strength at unirradiated condition is used for the calculation of the stress limit S_e. The Level-D criteria limit is estimated by multiplying the calculated S_e limit value with a safety factor of 2 to the as per the SDC-IC. In Figure 4, stress limits for Eurofer97 material are estimated and plotted.
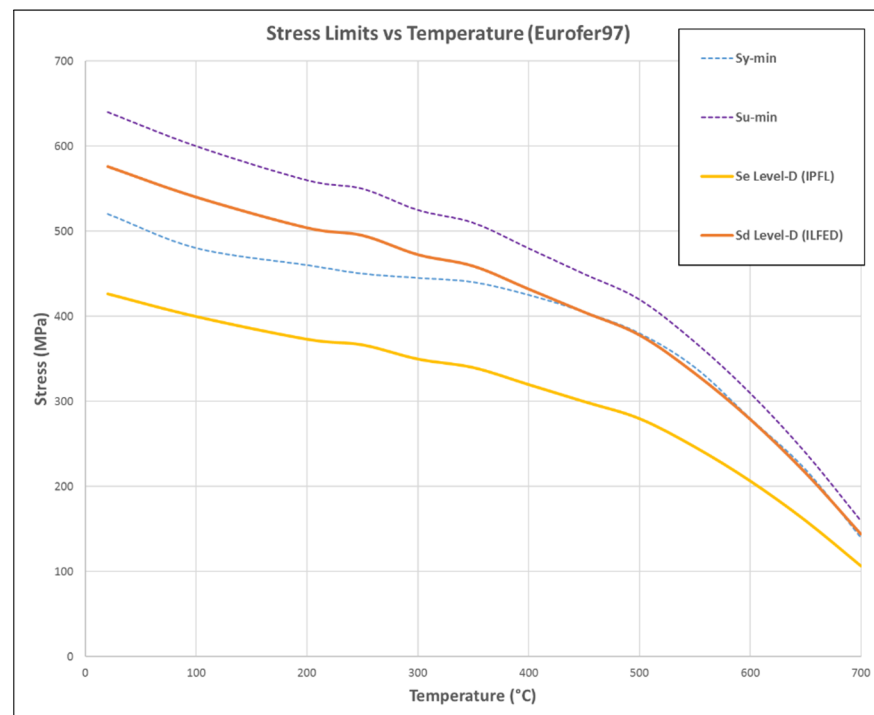

Figure 4. Stress limits with respect to temperature for Eurofer97 material.

The criterion for ILFED failure mode as per the RCC-MRx includes the peak stresses while SDC-IC recommends an additional criterion without incorporating the peak stresses [23,24].

$$\overline{P_L + P_B + Q + F} \ \leq \ S_{et} \ (RCC - MRx) \ and \ \overline{P_L + P_B + Q} \ \leq \ S_d \ (SDC - IC)$$

where the term $\overline{P_L + P_B + Q + F}$ represents the total primary plus secondary stress including the peak stresses and the term $\overline{P_L + P_B + Q}$ represents the total primary plus secondary stress excluding the peak stresses; S_{et} and S_d are the corresponding allowable total stress limits. Since the peak stresses in the FE solution can be affected by singularities and modelling approximations, it is decided to use the SDC-IC criteria without incorporating

the peak stresses for the present work. Similar to the calculation IPFL stress limits, it is decided to ignore the dependence on failure strain and the stress triaxiality on stress limit S_d for uniform strain values greater than 2%, and the limit values are calculated using the minimum tensile strength at the unirradiated condition. Resulting stress limits are plotted in Figure 4. A safety factor value of 1.35 is used to multiply S_d limit to estimate the Level-D criteria limit as per SDC-IC.

2.4. Nonlinear-Inelastic Structural Analysis

The nonlinear static-stress analysis is essentially carried out with the same boundary conditions and loads as in the previous linear static structural analysis. Additionally, two key changes are incorporated in the simulation settings: (1) Material nonlinearity defined using a classical von Mises plasticity-based hardening model and (2) geometric nonlinearity activated by turning on the large deflection parameter. Both of these changes essentially cause the stiffness matrix to be re-evaluated throughout the simulation accommodating the change in the material properties or the shape of the structure. As result, the model response becomes more realistic; however at the cost of demanding computational resources.

The tensile stress–strain curves for Eurofer97 are known to be affected by the irradiation. The irradiation hardening causes an increase in yield and tensile strengths with a corresponding loss of ductility characterized by the reduction in uniform and total elongation. However, this effect is reduced at temperatures above 350 °C, which is the operating range of HCPB BB [23,25]. Therefore, for the present work, tensile stress–strain curves at unirradiated conditions are used. It is assumed that this is the conservative stress–strain curve. However, due to the nonlinear nature of plastic deformation, in the future, the analysis could be repeated with stress–strain curves at different irradiated conditions when such data becomes available. Thus, a temperature-dependent, multi-linear plasticity is defined using the data from the uniaxial tension test at unirradiated conditions up to the point of uniform elongation, with perfect plasticity assumed after this point.

2.5. Assessment according to the Inelastic Criteria

The SDC-IC defines load factors and strain factors with which the primary and secondary loads should be multiplied for the assessment of the IPFL and ILFED failure modes. For the Level-D criteria, these factors are $\Gamma_L = 1.35$ (*mechanical − primary loads*) and $\Gamma_S = 1.0$ (*thermal − secondary loads*) for both IPFL and ILFED. Further, the SDC-IC defines the below criteria [24].

$$(\widetilde{\varepsilon}_m)_{pl} \leq \frac{\varepsilon_u(T_m, \Phi t_m)}{2} \text{ (IPFL) and } (\widetilde{\varepsilon})_{pl} \leq \frac{\varepsilon_{tr}(T, \Phi t)}{TF} \text{ (ILFED)}$$

where $(\widetilde{\varepsilon}_m)_{pl}$ and $(\widetilde{\varepsilon})_{pl}$ are the significant mean plastic strain and significant local plastic strain, respectively, which represent the greatest maximum principal strain values, evaluated from the corresponding strain tensors. $\varepsilon_u(T_m, \Phi t_m)$ is the minimum uniform elongation dependent on the thickness-averaged temperature, T_m and the thickness-averaged neutron fluence, Φt_m. Similarly, $\varepsilon_{tr}(T, \Phi t)$ is the minimum true strain at rupture dependent on the local temperature T and the local neutron fluence Φt. The parameter TF is the triaxiality factor defined as the ratio of Hydrostatic stress and von Mises stress normalized to unity for uniaxial loading, i.e., $TF = 3\sigma_H / \sigma_{vM}$. In Figure 5, the strain limits, ε_u and ε_{tr} for Eurofer97 material is estimated and plotted. Minimum saturation values of the irradiated properties are used in the temperature range of 20 °C to 350 °C. Unirradiated properties are used above 500 °C since the effect of irradiation is considered negligible above that temperature [25]. Values are linearly interpolated in the range between 350 °C to 500 °C.

The ILFED strain limits are further dependent on the stress triaxiality according to the SDC-IC criteria as mentioned above. This dependence is plotted in Figure 6. According to the equation, the limit strain values increase for TF values less than 1. However, it is thought that the void nucleation-dominated material failure at low triaxial values may not

be appropriately represented by the equation. Therefore, a constant limit value is used for *TF* values less than 1, which is assumed to be conservative in the range.
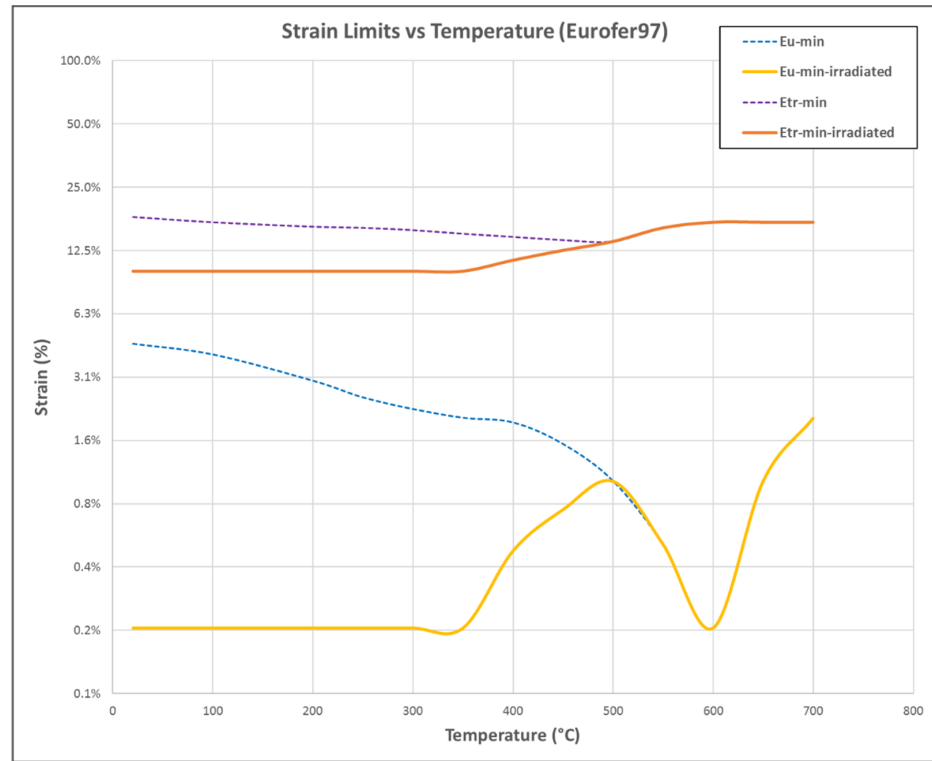

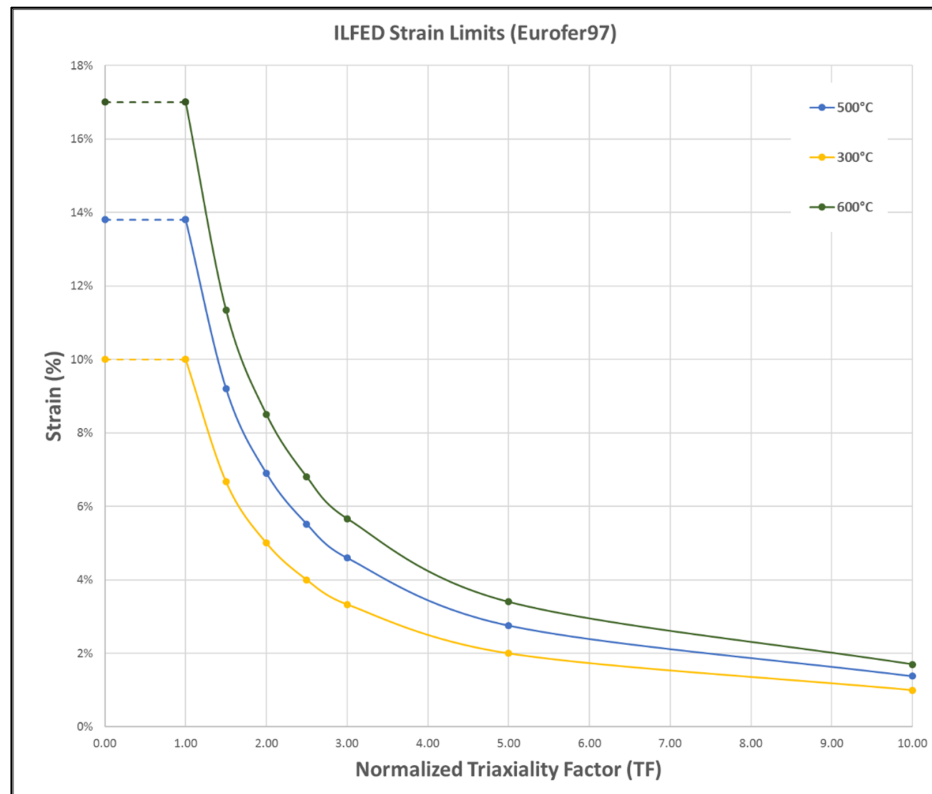**Figure 5.** Strain limits with respect to temperature for Eurofer97 material.

Figure 6. ILFED strain limits with respect to the triaxiality factor.

3. Results

From the thermal analysis, the temperature distribution of the BB cap region during normal operation is shown in Figure 7. It can be seen that the maximum temperature observed on the Eurofer structures is in the range of 300 °C to 576 °C with a localized peak temperature hot-spot on the middle section top region.
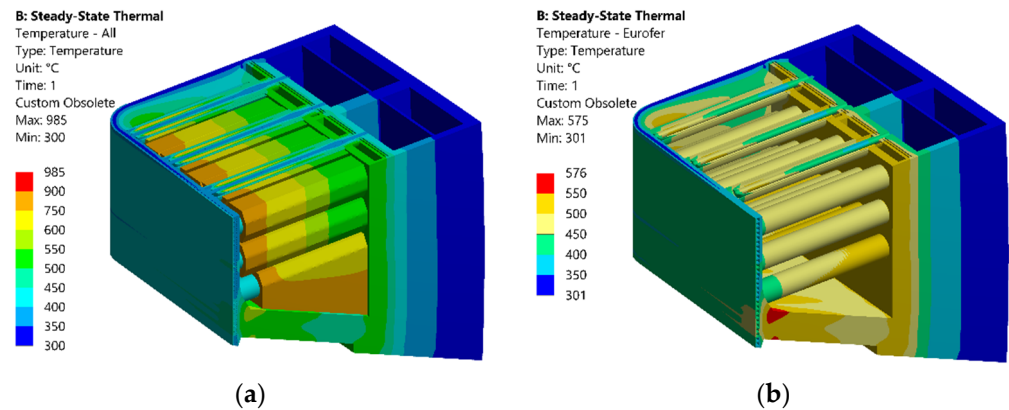

(**a**)   (**b**)

Figure 7. Temperature distribution (**a**) on the whole BB cap region, and (**b**) on Eurofer97 structures.

3.1. Elastic Analysis Results and Assessment

The von Mises stress distribution of the structural components in the BB cap region is plotted in Figure 8. After neglecting the non-physical stress concentrations near the boundary conditions and the bonded contact regions, it is observed that some locations of the *first wall*, *breeder pins*, and *tubes* are under relatively high stress (>350 MPa). The assessment following the elastic criteria for IPFL and ILFED damage modes is performed at a few selected locations and the results are presented in Table 1. Safety margins for both criteria are estimated as (Stress Limit—linearized stress value)/Stress Limit and expressed as a percentage. Identified high stressed regions and components are shown in Figure 9. It can be seen that both IPFL and ILFED margins are not satisfied in regions of *first wall* and *breeder pins*. Due to coolant flow with a large temperature range, there are high thermal gradients between the components. The resulting secondary thermal stresses increase the total stresses higher than the elastic margins recommended by the elastic criteria.

Table 1. Assessment against IPFL and ILFED damage modes according to elastic criteria.

Part	Loc.	$T_{average}$ (°C)	$\overline{P_L+Q_L}$ (MPa)	S_e^D (MPa)	IPFL Margin (%)	T_{point} (°C)	$\overline{P_L+P_b+Q}$ (MPa)	S_d^D (MPa)	ILFED Margin (%)
Cap Top	A	480	68	287	76%	514	211	388	46%
	B	488	39	283	86%	521	199	382	48%
	C	465	201	295	32%	466	300	398	25%
	D	471	276	292	5%	474	308	394	22%
	E	384	282	329	14%	386	311	444	30%
	F	551	94	244	62%	572	104	330	68%
	G	518	167	269	38%	524	237	354	33%

Table 1. *Cont.*

Part	Loc.	$T_{average}$ (°C)	$\overline{P_L+Q_L}$ (MPa)	S_e^D (MPa)	IPFL Margin (%)	T_{point} (°C)	$\overline{P_L+P_b+Q}$ (MPa)	S_d^D (MPa)	ILFED Margin (%)
First Wall	A	338	740	342	Failed	351	801	462	Failed
	B	341	569	341	Failed	353	584	460	Failed
	C	381	576	330	Failed	380	585	445	Failed
	D	386	573	328	Failed	388	598	443	Failed
	E	397	300	324	7%	401	339	438	23%
	F	370	443	333	Failed	370	446	450	1%
	G	390	331	327	Failed	396	378	441	14%
	H	391	341	326	Failed	397	354	441	20%
	I	495	333	279	Failed	496	359	377	5%
	J	384	272	329	17%	395	338	444	24%
Back Plate	A	511	229	270	15%	514	241	364	34%
	B	523	149	262	43%	524	169	354	52%
	C	516	187	267	30%	516	253	360	30%
BSS	A	516	210	267	21%	516	284	360	21%
	B	514	222	268	17%	514	276	362	24%
Pressure Tubes	A	414	299	318	6%	414	363	429	15%
	B	441	328	306	Failed	446	333	413	20%
	C	442	316	306	Failed	446	321	413	22%
	D	409	273	320	15%	410	294	431	32%
Breeder Pins	A	500	920	276	Failed	499	1006	373	Failed
	B	517	354	266	Failed	517	372	359	Failed
	C	517	366	266	Failed	517	395	359	Failed
	D	516	360	267	Failed	515	393	360	Failed
	E	518	337	265	Failed	518	348	358	3%
	F	516	436	267	Failed	516	451	360	Failed
	G	518	285	265	Failed	518	309	358	14%
	H	509	788	271	Failed	508	880	366	Failed
	I	506	926	273	Failed	506	1015	368	Failed

3.2. Inelastic Analysis Results and Assessment

The maximum principal plastic strain values on the BB cap region structural components from the inelastic simulation results are plotted in Figure 10. The pattern of the stress contour is similar to the linear analysis. It can be also seen that some locations in the *first wall* and *breeder pins* are under relatively high plastic strain. Assessment following the inelastic criteria in Section 2.5 is performed for the IPFL and ILFED damage modes and the results are presented in Table 2. Similar to the elastic assessment, safety margins for IPFL criteria are estimated by comparing the linearized strain values with the corresponding strain limit. In order to estimate the ILFED safety margin, the local strain values are multiplied by the corresponding stress triaxiality factor—TF, and then compared with the uniaxial strain limits. The distribution of the TF contour is plotted in Figure 11. Due to the

reasons explained in Section 2.4, TF values less than 1 are increased so that the minimum value of TF remains 1.
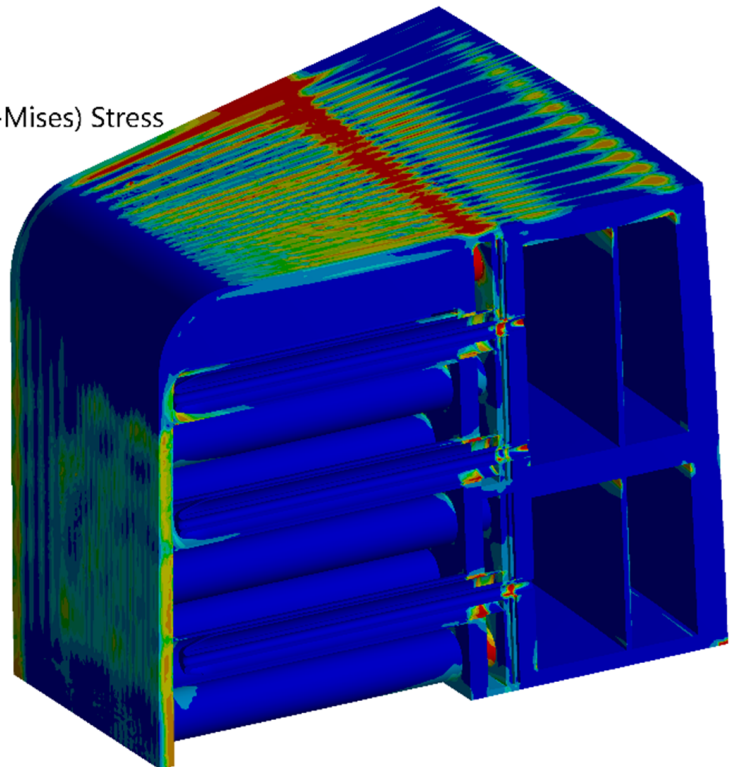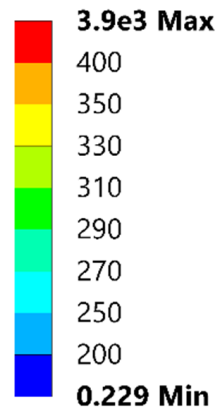

Figure 8. Von Mises stress results contour on BB cap region—elastic analysis.
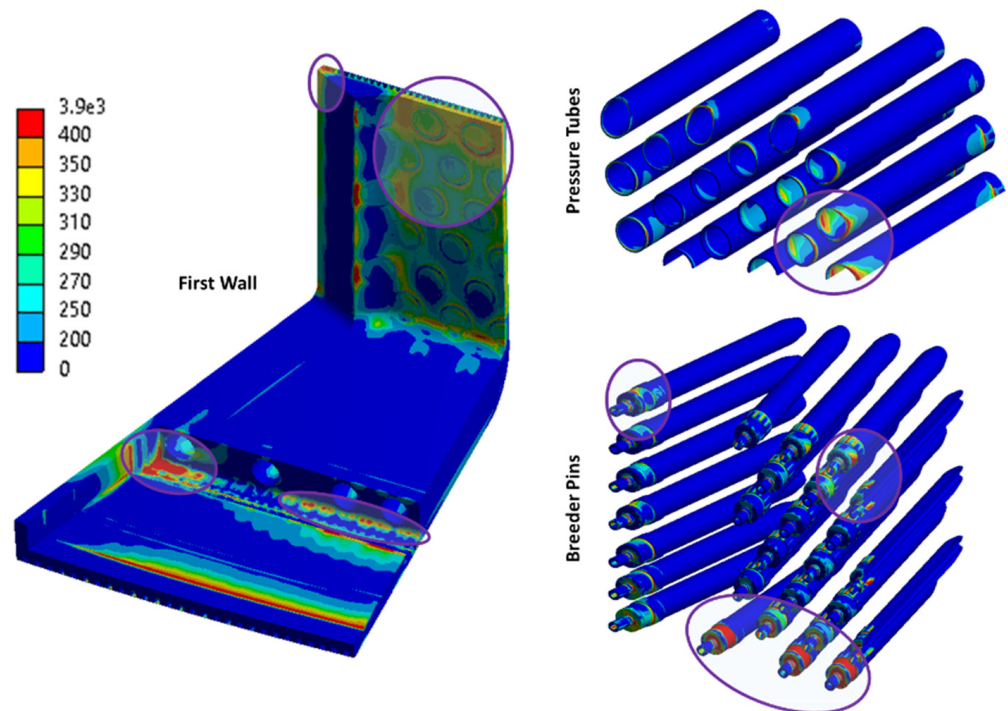

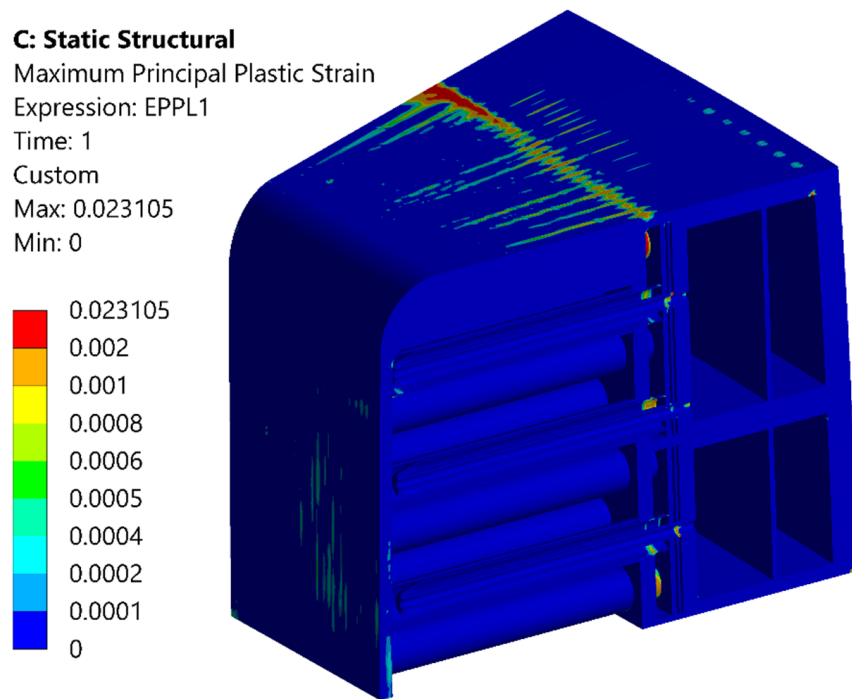**Figure 9.** Identified high stressed locations according to elastic assessment.

Figure 10. Maximum principal strain contour on BB cap region—inelastic analysis.

Table 2. Assessment against IPFL and ILFED damage modes according to inelastic criteria.

Part	Loc.	$T_{average}$ (°C)	$(\tilde{\varepsilon}_m)_{pl}$ (%)	$\frac{\varepsilon_u}{2}$ (%)	IPFL Criteria Margin	T_{point} (°C)	$(\tilde{\varepsilon})_{pl} \times TF$ (%)	ε_{tr} (%)	ILFED Criteria Margin
Cap Top	A	480	0.0005%	0.4475%	100%	514	0.01%	14.60%	100%
	B	488	0.0010%	0.4692%	100%	521	0.02%	14.83%	100%
	C	465	0.0010%	0.4076%	100%	466	0.00%	13.00%	100%
	D	471	0.0001%	0.4230%	100%	474	0.00%	13.26%	100%
	E	384	0.0000%	0.1915%	100%	386	0.00%	10.76%	100%
	F	551	0.0000%	0.2461%	100%	572	0.00%	16.38%	100%
	G	518	0.0000%	0.4006%	100%	524	0.00%	14.92%	100%
First Wall	A	338	0.5416%	0.1000%	Failed	351	0.84%	10.16%	92%
	B	341	0.2048%	0.1000%	Failed	353	0.33%	10.19%	97%
	C	381	0.2736%	0.1815%	Failed	380	0.34%	10.63%	97%
	D	386	0.2676%	0.1965%	Failed	388	0.29%	10.80%	97%
	E	397	0.0036%	0.2245%	98%	401	0.01%	11.10%	100%
	F	370	0.0502%	0.1534%	67%	370	0.05%	10.45%	99%
	G	390	0.0100%	0.2065%	95%	396	0.06%	10.98%	99%
	H	391	0.0092%	0.2091%	96%	397	0.06%	11.01%	99%
	I	495	0.0000%	0.4870%	100%	496	0.00%	14.00%	100%
	J	384	0.0072%	0.1895%	96%	395	0.08%	10.96%	99%

Table 2. *Cont.*

Part	Loc.	$T_{average}$ (°C)	$(\tilde{\varepsilon}_m)_{pl}$ (%)	$\frac{\varepsilon_u}{2}$ (%)	IPFL Criteria Margin	T_{point} (°C)	$(\tilde{\varepsilon})_{pl} \times TF$ (%)	ε_{tr} (%)	ILFED Criteria Margin
Back Plate	A	511	0.0000%	0.4374%	100%	514	0.00%	14.60%	100%
	B	523	0.0000%	0.3702%	100%	524	0.00%	14.92%	100%
	C	516	0.0000%	0.4108%	100%	516	0.00%	14.66%	100%
BSS	A	516	0.0000%	0.4084%	100%	516	0.00%	14.66%	100%
	B	514	0.0000%	0.4197%	100%	514	0.00%	14.60%	100%
Pressure Tubes	A	414	0.0060%	0.2706%	98%	414	0.04%	11.43%	100%
	B	441	0.0014%	0.3436%	100%	446	0.01%	12.36%	100%
	C	442	0.0000%	0.3456%	100%	446	0.00%	12.36%	100%
	D	409	0.0012%	0.2581%	100%	410	0.01%	11.33%	100%
Breeder Pins	A	500	0.3824%	0.4993%	23%	499	0.42%	14.10%	97%
	B	517	0.1057%	0.4028%	74%	517	0.13%	14.69%	99%
	C	517	0.2214%	0.4020%	45%	517	0.28%	14.69%	98%
	D	516	0.0655%	0.4108%	84%	515	0.08%	14.63%	99%
	E	518	0.0913%	0.3978%	77%	518	0.10%	14.73%	99%
	F	516	0.1854%	0.4094%	55%	516	0.19%	14.66%	99%
	G	518	0.0000%	0.3973%	100%	518	0.00%	14.73%	100%
	H	509	0.2996%	0.4487%	33%	508	0.32%	14.40%	98%
	I	506	0.4854%	0.4626%	Failed	506	0.50%	14.33%	97%

C: Static Structural
TF_SDC_IC
Expression: TF = ((S1+S2+S3)/(SEQV))+((1-((S1+S2+S3)/(SEQV)))+abs(1-((S1+S2+S3)/(SEQV))))/2
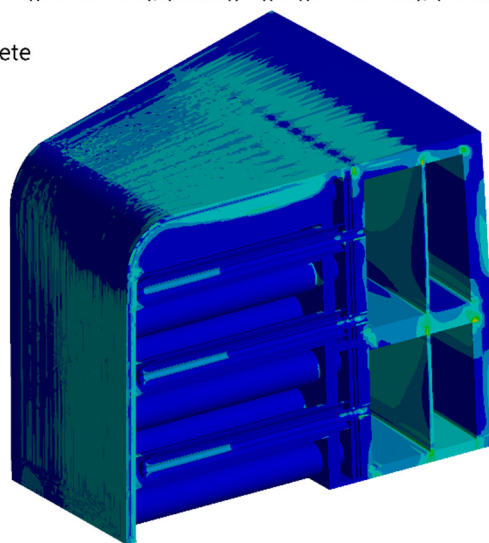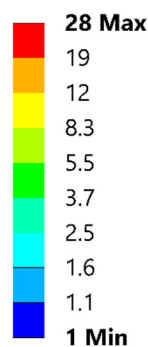Time: 1
Custom Obsolete

28 Max
19
12
8.3
5.5
3.7
2.5
1.6
1.1
1 Min

Figure 11. Stress triaxiality contour on BB cap region—inelastic analysis.

4. Discussion

By comparing the results from both elastic and inelastic assessments, it can be seen that the elastic criteria provide a too conservative estimate of the design safety. Compared

to normal ductile materials, Eurofer97 has a limited strain-hardening capability, but the material retains considerable ductility after necking. The elastic design-by-analysis code does not take this factor into account. Consequently, the stress limits derived from the ultimate tensile strength values for the elastic assessment are affected by the lack of strain hardening capability of Eurofer97. Particularly for the IPFL damage mode, the stress limits are much below the yield point as shown in Figure 4. Corresponding inelastic assessment is based on the plastic strain limits and hence it is not affected by this problem. This is reflected in the improved assessment results for IPFL damage mode using the inelastic criteria.

For the inelastic assessment of ILFED damage mode, the strain limits are derived from the total elongation values (true strain at rupture), which remain high for Eurofer97 even at irradiated conditions. As a result, these limits are never crossed in simulation. It should be noted that the linear safety margins calculated from the inelastic assessment results cannot properly represent the nonlinear behavior involved. For example, a small increase in primary loads could induce plastic instability in the structure and rapidly consume the calculated linear strain safety margin in the structure.

5. Conclusions and Outlook

The nonlinear inelastic and elastic analyses on the cap region of HCPB BB have been conducted. Assessments following the inelastic route and elastic route show that the inelastic assessment could help to reduce the conservatism in the design of Eurofer structures. Specific to the HCPB BB structure that is dominated by the temperature-driven secondary loads, it still needs to be decided whether IPFL damage limits based on the uniaxial uniform strain values are appropriate in comparison to the ILFED damage limits. Nevertheless, there remain many assumptions that need to be addressed in further studies to confidently move forward. Some of these are listed out below:

- Material hardening behavior after the uniform strain point is not precisely known. Conventional uniaxial tension test data is affected by the necking at the uniform strain point and may not be valid after necking. Since Eurofer material has very low uniform strain even at unirradiated conditions, the hardening behavior at higher strains needed to be understood.
- It is assumed that the failure strain–triaxial relationship for Eurofer is as represented in Figure 6, estimated from the equation for SDC-IC ILFED criteria. However, it is known that this equation may not properly represent the material failure dominated by void nucleation at low triaxiality values as opposed to the failure dominated by void growth at high triaxiality. Even at high triaxiality values, the relationship needs to be verified for Eurofer97 material.
- As described in Section 2.4, the work here is performed using tensile stress–strain data at unirradiated conditions. Since at irradiated conditions, the yield stress and ultimate stress increases due to hardening, it is assumed that the unirradiated stress–strain curve is conservative. However, the plastic flow localization is an instability phenomenon and hence it could be affected by any change in the hardening behavior.
- For the HCPB BB, component level tests under similar operating conditions (high secondary-thermal loads combined with relatively low primary loads) could be performed to validate the applicability of IPFL damage limits against the more relaxed ILFED damage limits.

References

1. Donné, A.J.H. The European Roadmap towards Fusion Electricity. *Philos. Trans. R. Soc. Math. Phys. Eng. Sci.* **2019**, *377*, 20170432. [CrossRef]
2. Federici, G.; Boccaccini, L.V.; Cismondi, F.; Gasparotto, M.; Poitevin, Y.; Ricapito, I. An Overview of the EU Breeding Blanket Design Strategy as an Integral Part of the DEMO Design Effort. *Fusion Eng. Des.* **2019**, *141*, 30–42. [CrossRef]
3. Raffray, A.R.; Calcagno, B.; Chappuis, P.; Fu, Z.; Furmanek, A.; Jiming, C.; Kim, D.-H.; Khomiakov, S.; Labusov, A.; Martin, A.; et al. The ITER Blanket System Design Challenge. *Nucl. Fusion* **2014**, *54*, 033004. [CrossRef]
4. Hernández, F.A.; Pereslavtsev, P.; Zhou, G.; Kang, Q.; D'Amico, S.; Neuberger, H.; Boccaccini, L.V.; Kiss, B.; Nádasi, G.; Maqueda, L.; et al. Consolidated Design of the HCPB Breeding Blanket for the Pre-Conceptual Design Phase of the EU DEMO and Harmonization with the ITER HCPB TBM Program. *Fusion Eng. Des.* **2020**, *157*, 111614. [CrossRef]
5. Cismondi, F.; Kecskes, S.; Aiello, G. HCPB TBM Thermo Mechanical Design: Assessment with Respect Codes and Standards and DEMO Relevancy. *Fusion Eng. Des.* **2011**, *86*, 2228–2232. [CrossRef]
6. Hernández, F.; Cismondi, F.; Kiss, B. Thermo-Mechanical Analyses and Assessment with Respect to the Design Codes and Standards of the HCPB-TBM Breeder Unit. *Fusion Eng. Des.* **2012**, *87*, 1111–1117. [CrossRef]
7. Zhou, G.; Hernández, F.; Boccaccini, L.V.; Chen, H.; Ye, M.Y. Preliminary Structural Analysis of the New HCPB Blanket for EU DEMO Reactor. *Int. J. Hydrog. Energy* **2016**, *41*, 7053–7058. [CrossRef]
8. Zhou, G.; Hernández, F.; Boccaccini, L.V.; Chen, H.; Ye, M.Y. Preliminary Steady State and Transient Thermal Analysis of the New HCPB Blanket for EU DEMO Reactor. *Int. J. Hydrog. Energy* **2016**, *41*, 7047–7052. [CrossRef]
9. Hernández, F.; Pereslavtsev, P.; Kang, Q.; Norajitra, P.; Kiss, B.; Nádasi, G.; Bitz, O. A New HCPB Breeding Blanket for the EU DEMO: Evolution, Rationale and Preliminary Performances. *Fusion Eng. Des.* **2017**, *124*, 882–886. [CrossRef]
10. Zhou, G.; Hernández, F.; Boccaccini, L.V.; Chen, H.; Ye, M. Design Study on the New EU DEMO HCPB Breeding Blanket: Thermal Analysis. *Prog. Nucl. Energy* **2017**, *98*, 167–176. [CrossRef]
11. Zhou, G.; Hernández, F.A.; Zeile, C.; Maione, I.A. Transient Thermal Analysis and Structural Assessment of an Ex-Vessel LOCA Event on the EU DEMO HCPB Breeding Blanket and the Attachment System. *Fusion Eng. Des.* **2018**, *136*, 34–41. [CrossRef]
12. Zeile, C.; Hernández, F.A.; Maione, I.A.; Zhou, G.; Bachmann, C. Structural Assessment of the HCPB Breeding Blanket Segments in the EU DEMO Reactor under Normal Operation and a Central Plasma Disruption. *Fusion Eng. Des.* **2018**, *136*, 335–339. [CrossRef]
13. Hernández, F.; Arbeiter, F.; Boccaccini, L.V.; Bubelis, E.; Chakin, V.; Cristescu, I.; Ghidersa, B.-E.; Gonzalez, M.; Hering, W.; Hernandez, T.; et al. Overview of the HCPB Research Activities in EUROfusion. *IEEE Trans. Plasma Sci.* **2018**, *46*, 2247–2261. [CrossRef]
14. Zhou, G.; Hernández, F.; Zeile, C. A Methodology for Thermo-Mechanical Assessment of in-Box LOCA Events on Fusion Blankets and Its Application to EU DEMO HCPB Breeding Blanket. *Kerntechnik* **2018**, *83*, 256–260. [CrossRef]
15. Aktaa, J.; Kecskés, S.; Cismondi, F. Non-Linear Failure Analysis of HCPB Test Blanket Module. *Fusion Eng. Des.* **2012**, *87*, 1085–1090. [CrossRef]
16. Aktaa, J.; Kecskés, S.; Pereslavtsev, P.; Fischer, U.; Boccaccini, L.V. Non-Linear Failure Analysis of HCPB Blanket for DEMO Taking into Account High Dose Irradiation. *Fusion Eng. Des.* **2014**, *89*, 1664–1668. [CrossRef]
17. Aktaa, J.; Carin, Y.; Vallory, J. Non-Linear Assessment of Critical Failure Modes in the First Wall of the European TBM. *Fusion Eng. Des.* **2018**, *128*, 223–230. [CrossRef]
18. Jin, X.Z. Preliminary Safety Analysis of LOCAs in One EU DEMO HCPB Blanket Module. *Fusion Eng. Des.* **2017**, *124*, 1233–1236. [CrossRef]
19. Stonehouse, M.; Seipp, T.G.; Kanamaru, S.; Morrison, S. A Novel Comparison of Design-by-Analysis Methods. *J. Press. Vessel. Technol.* **2012**, *134*, 054502-1–054502-4. [CrossRef]
20. Zhu, X.-K. Strength Criteria Versus Plastic Flow Criteria Used in Pressure Vessel Design and Analysis. *J. Press. Vessel. Technol.* **2016**, *138*, 041402-1–041402-7. [CrossRef]

21. Fursdon, M.; You, J.-H.; Li, M. Towards Reliable Design-by-Analysis for Divertor Plasma Facing Components—Guidelines for Inelastic Assessment (Part 1: Unirradiated). *Fusion Eng. Des.* **2019**, *147*, 111234. [CrossRef]
22. Fursdon, M.; You, J.-H.; Barrett, T.; Li, M. A Hybrid Analysis Procedure Enabling Elastic Design Rule Assessment of Monoblock-Type Divertor Components. *Fusion Eng. Des.* **2018**, *135*, 154–164. [CrossRef]
23. AFCEN. *RCC-MRx 2012: Design and Construction Rules for Mechanical Components of Nuclear Installations. Addenda Included*; AFCEN: Courbevoie, France, 2013.
24. ITER. *SDC-IC: Structural Design Criteria for In-vessel Components*; ITER: Saint-Paul-lès-Durance, France, 2012.
25. Aiello, G.; Aktaa, J.; Cismondi, F.; Rampal, G.; Salavy, J.-F.; Tavassoli, F. Assessment of Design Limits and Criteria Requirements for Eurofer Structures in TBM Components. *J. Nucl. Mater.* **2011**, *414*, 53–68. [CrossRef]